

 Open access • Posted Content • DOI:10.1101/186767

## A rainfall-manipulation experiment with 517 *Arabidopsis thaliana* accessions

— [Source link](#) 

Moises Exposito-Alonso, R Rodríguez Gómez, Cristina A. Barragan, Giovanna Capovilla ...+34 more authors

**Institutions:** Max Planck Society, Technical University of Madrid, University of Tübingen

**Published on:** 10 Sep 2017 - [bioRxiv](#) (bioRxiv)

Related papers:

- [1,135 ionomes reveal the global pattern of leaf and seed mineral nutrient and trace element diversity in \*Arabidopsis thaliana\*.](#)
- [Expanding ecological and evolutionary insights from wild \*Arabidopsis thaliana\* accessions.](#)
- [Full species-wide leaf and seed ionic diversity of \*Arabidopsis thaliana\*](#)
- [Separating the wheat from the chaff – a strategy to utilize plant genetic resources from ex situ genebanks](#)
- [Genome-wide scans of selection highlight the impact of biotic and abiotic constraints in natural populations of the model grass \*Brachypodium distachyon\*.](#)

Share this paper:    

View more about this paper here: <https://typeset.io/papers/a-rainfall-manipulation-experiment-with-517-arabidopsis-3mklckon8m>

# 1 A rainfall-manipulation experiment with 517

## 2 *Arabidopsis thaliana* accessions

3 Moises Exposito-Alonso<sup>1</sup>, Rocío Gómez Rodríguez<sup>2</sup>, Cristina Barragán<sup>1</sup>, Giovanna Capovilla<sup>1</sup>, Eunyoung Chae<sup>1</sup>,  
4 Jane Devos<sup>1</sup>, Ezgi S. Dogan<sup>1</sup>, Claudia Friedemann<sup>1</sup>, Caspar Gross<sup>1</sup>, Patricia Lang<sup>1</sup>, Derek Lundberg<sup>1</sup>, Vera  
5 Middendorf<sup>1</sup>, Jorge Kageyama<sup>1</sup>, Talia Karasov<sup>1</sup>, Sonja Kersten<sup>1</sup>, Sebastian Petersen<sup>1</sup>, Leily Rabbani<sup>1</sup>, Julian  
6 Regalado<sup>1</sup>, Lukas Reinelt<sup>1</sup>, Beth Rowan<sup>1</sup>, Danelle K. Seymour<sup>1</sup>, Efthymia Symeonidi<sup>1</sup>, Rebecca Schwab<sup>1</sup>, Diep  
7 Thi Ngoc Tran<sup>1</sup>, Kavita Venkataramani<sup>1</sup>, Anna-Lena Van de Weyer<sup>1</sup>, François Vasseur<sup>1</sup>, George Wang<sup>1</sup>, Ronja  
8 Wedegärtner<sup>1</sup>, Frank Weiss<sup>1</sup>, Rui Wu<sup>1</sup>, Wanyan Xi<sup>1</sup>, Maricris Zaidem<sup>1</sup>, Wangsheng Zhu<sup>1</sup>, Fernando  
9 García-Arenal<sup>2</sup>, Hernán A. Burbano<sup>1</sup>, Oliver Bossdorf<sup>3</sup>, Detlef Weigel<sup>1\*</sup>.

10 <sup>1</sup> Department of Molecular Biology, Max Planck Institute for Developmental Biology, Tübingen, Germany

11 <sup>2</sup> Center for Plant Biotechnology and Genomics, Technical University of Madrid, Pozuelo de Alarcón, Spain

12 <sup>3</sup> Institute of Ecology and Evolution, University of Tübingen, Tübingen, Germany

13 \* correspondence to: [weigel@weigelworld.org](mailto:weigel@weigelworld.org)

14 Running title: A Climate Change Experiment with *A. thaliana*

15 Keywords: *Arabidopsis thaliana*, Climate Change, Field experiment, Local adaptation.

16 **The gold standard for studying natural selection and adaptation in the wild is to quantify lifetime**  
17 **fitness of individuals from natural populations that have been grown together in a common garden,**  
18 **or that have been reciprocally transplanted. By combining fitness values with species traits and**  
19 **genome sequences, one can infer selection coefficients at the genetic level. Here we present a**  
20 **rainfall-manipulation experiment with 517 whole-genome sequenced natural accessions of the**  
21 **plant *Arabidopsis thaliana* spanning the global distribution of the species. The experiments were**  
22 **conducted in two field stations in contrasting climates, in the Mediterranean and in Central Europe,**  
23 **where we built rainout shelters and simulated high and low rainfall. Using custom image analysis**  
24 **we quantified fitness- and phenology-related traits for 23,154 pots, which contained about 14,500**  
25 **plants growing independently, and over 310,000 plants growing in small populations (max. 30**  
26 **plants). This large field experiment dataset, which associates fitness and ecologically-relevant traits**  
27 **with genomes, will provide an important resource to test eco-evolutionary genetic theories and to**  
28 **understand the potential evolutionary impacts of future climates on an important plant model**  
29 **species.**

## 30 **Background and Summary**

31 Darwin's theory of evolution by natural selection states that when individuals of a population have distinct  
32 traits that improve their ability to survive and reproduce, and these are heritable, the population will change  
33 and adapt over generations<sup>1</sup>. This was formally described by R. A. Fisher<sup>2</sup>, stating that the higher the genetic  
34 variance in fitness, the higher the rate of adaptation of a species. Natural selection over morphological,  
35 physiological or other traits has been studied in a wide range of organisms<sup>3-6</sup> using observational and  
36 experimental fitness measurements of multiple individuals in field conditions. However, studies that combine  
37 such measurements with knowledge on genome-wide variation are, in comparison, very rare<sup>7-9</sup>. This is  
38 surprising, given that they can enable the translation of selection coefficients to the genetic level and thus  
39 ultimately help us to understand whether traits will evolve over generations.

40 With climate change, the study of adaptation to the environment has acquired new importance.  
41 Predictions of climate change indicate not only that temperature will rise, but that also precipitation regimes  
42 will be altered, leading to more frequent and extreme droughts<sup>10</sup>, posing the critical question of whether  
43 populations will be able to adapt or will become extinct<sup>11</sup>. Field experiments where climate variables such as  
44 rainfall are manipulated can be used to address this question<sup>12</sup>.

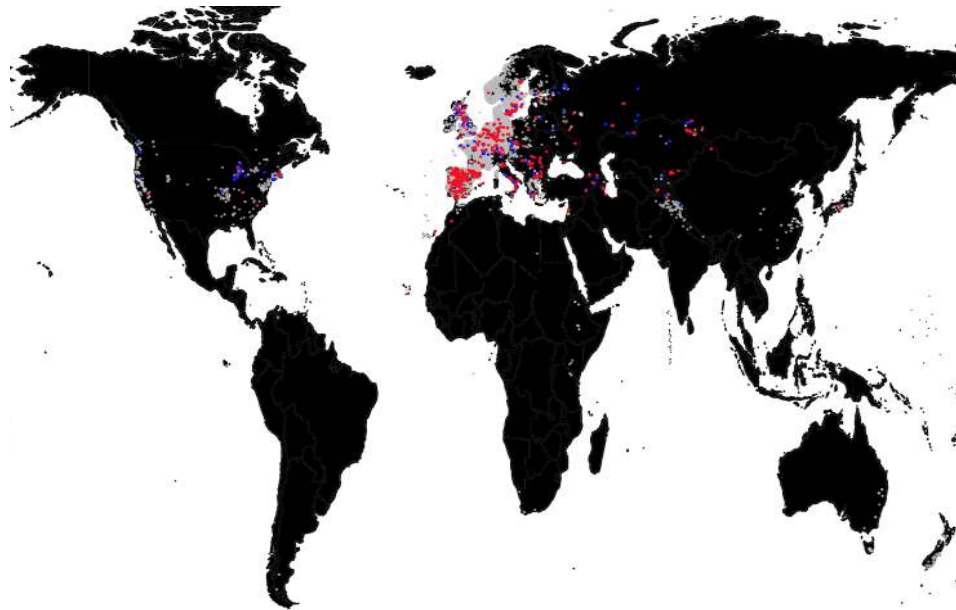
45 Here we present a high-throughput field experiment with 517 whole-genome sequenced natural lines  
46 of *Arabidopsis thaliana*<sup>13</sup> grown under rainfall-manipulation conditions at two field stations with contrasting

47 climate. This experiment was designed to be of a sufficiently large scale to enable powerful genome-wide  
48 association analyses<sup>14</sup> and to maximize the replicability of species-wide patterns, which increases with the  
49 diversity of genotypes included in an experiment<sup>15</sup>. This dataset will be invaluable for the study of natural  
50 selection and adaptation in the context of global climate change at the genetic level<sup>16</sup>, building on the genetic  
51 catalog of the 1001 Genomes Project<sup>13</sup> and complementing the already published extensive set of traits  
52 measured in controlled growth chamber or greenhouse conditions<sup>17,18</sup>.

## 53 **Methods**

### 54 **Accessions from the 1001 Genomes Project**

55 The 1001 Genomes (1001G) Project<sup>13</sup> has provided information on 1,135 natural lines or accessions and  
56 11,769,920 SNPs and small indels called after re-sequencing (Fig. 1). To select the most genetically and  
57 geographically informative 1001G lines, we applied several filters: (1) First we removed the accessions with the  
58 lowest genome quality. We discarded those with < 10X genome coverage of Illumina sequencing reads and <  
59 90% congruence of SNPs called from MPI and GMI pipelines<sup>13</sup>. (2) We removed near-identical individuals.  
60 Using Plink<sup>19</sup> we computed identity by state across the 1,135 accessions. For pairs of accessions with < 0.01  
61 differences per SNP (<100,000 variants approx.), we randomly selected one accession to include in our study.  
62 (3) Finally, we reduced geographic sampling ascertainment bias, as the sampling for 1001G was performed in  
63 neither a random nor a regularly structured scheme. Some laboratories provided several lines per location  
64 whereas others provided lines that were collected at least several hundred kilometres apart. Using each  
65 accession's collection location, we computed Euclidean distances across the 1,135 accessions and identified all  
66 pairs that were apart less than 0.0001 Euclidean distance in degrees latitude and longitude (<< 100 meters).  
67 From such pairs, we randomly selected one accession to remain. After applying criteria (1), (2), and (3), we  
68 obtained a final set of 523 accessions ([Datasets 1 and 2](#)). To bulk seeds for our rainfall-manipulation  
69 experiment and control for maternal effects, we first propagated accessions in controlled conditions. We  
70 stratified the seeds one week at 4°C, we sowed them in trays with industrial soil (CL-P, Einheitserde  
71 Werkverband e. V., Sinntal-Altengronau Germany) and placed them in a growth room with 16 h light and 23°C  
72 for one week. Trays were vernalized for 60 days at 4°C and 8h daylength. After vernalization, trays were moved  
73 back to 16 h light and 23°C for final growth and reproduction. This generated sufficient seeds for 517  
74 accessions, which were later grown in the field in two locations ([Fig. 1](#)). Seeds originating from the same  
75 parents can be ordered from the 1001G seed stock at the Arabidopsis Biological Resource Center (CS78942).



76 **Figure 1. Geographic distribution of accessions.** Locations of *Arabidopsis thaliana* accessions used in this experiment  
77 (red), 1001G accessions (blue), and all sightings of the species in [gbif.org](http://gbif.org) (grey).

## 78 **Field experiment design**

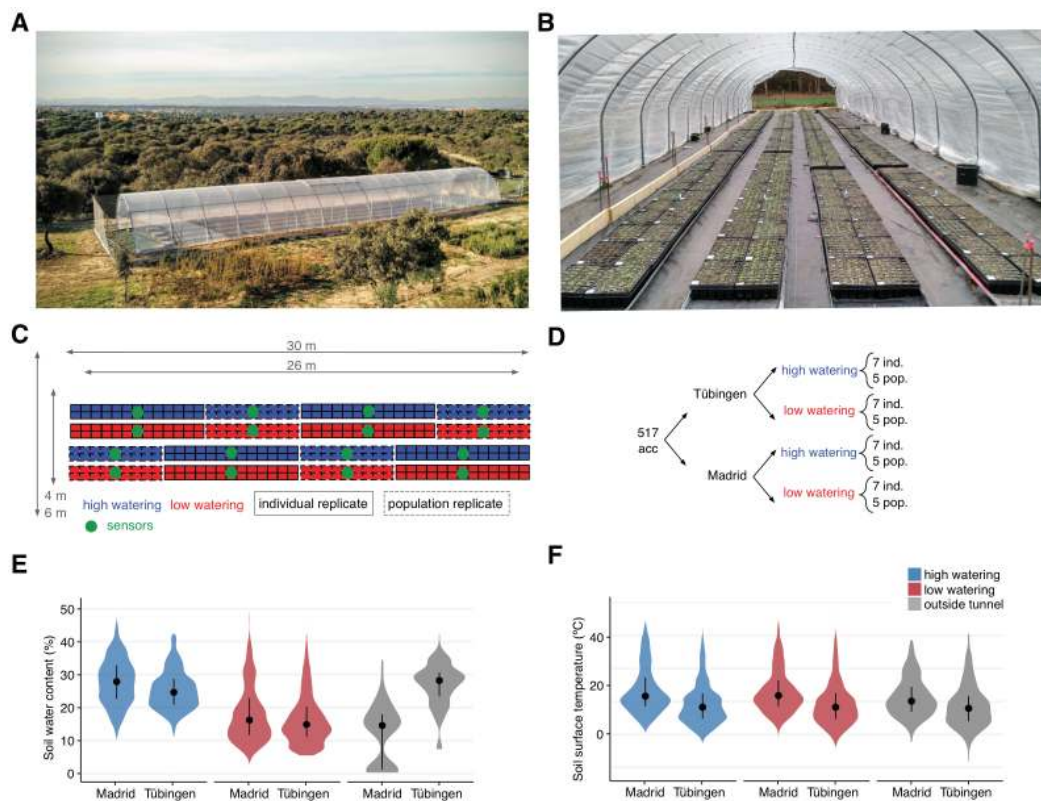
### 79 Rainout shelter design

80 We built two 30 m x 6 m tunnels of PVC plastic foil to fully exclude rainfall in Madrid (Spain, [40.40805°N](https://www.google.com/maps/place/40.40805%N+-3.83535%E)  
81 [-3.83535°E](https://www.google.com/maps/place/48.545809%N+9.042449%E)) and in Tübingen (Germany, [48.545809°N 9.042449°E](https://www.google.com/maps/place/48.545809%N+9.042449%E)) (Fig. 2). The foil tunnels are different from a  
82 regular greenhouse in that they are completely open on two sides. Thus, ambient temperatures vary virtually  
83 as much as outside the foil shelter (see Environmental sensors section). In each location, we supplied artificial  
84 watering in two contrasting regimes: abundant watering and reduced watering. Inside each tunnel, we created  
85 a 4% slope, and four flooding tables (1 m x 25 m, Hellmuth Bahrs GmbH & Co KG, Brüggem, Germany) covered  
86 with soaking mats (4 l/m<sup>2</sup>, Gärtnereinkauf Münchingen GmbH, Münchingen, Germany) were placed on the  
87 ground in parallel to the slope. Water was able to drain at the lower end of the flooding table (Fig. 2). A  
88 watering gun was used to manually simulate rainfall from the top.

89 For sowing, we used potting trays with 8x5 cells (5.5 cm x 5.5 cm x 10 cm size) and industrial soil (CL-P,  
90 Einheitserde Werkverband e.V., Sinntal-Altengronau Germany). One genotype was sown per cell, excluding  
91 corner cells, to avoid extreme edge effects. We grew a total of 12 replicates per genotype per treatment: Five  
92 replicates were sown at high density, with 30 seeds per cell and without further intervention (“population  
93 replicate”). The remaining seven replicates were planted at low density (ca. 10 seeds) and one seedling was  
94 selected at random after germination (“individual replicate”). Excess individuals were culled. While the

95 population replicates should more faithfully reflect survival from seed to reproduction, the individual replicates  
 96 were useful to more accurately monitor flowering time and seed set.

97 We used a randomized incomplete block design (Fig. 2). One block of the 517 genotypes spanned  
 98 14.36 trays (36 cells/tray), and genotypes were randomized within each block. The design was identical in  
 99 Madrid and Tübingen (Fig. 2).



100 **Figure 2. Field experiment design.** (A) Aerial view of foil tunnel settings in Madrid and (B) view inside the foil tunnel in  
 101 Tübingen. (C) Spatial distribution of blocks and replicates and (D) experimental design. (E) Soil water content and (F) soil  
 102 surface temperature from the 34 sensors monitoring each experimental block and conditions outside the tunnel.

103 Environmental sensors

104 Environmental variables — air temperature, photosynthetically active radiation (PAR) and soil water content —  
 105 were monitored every 15 minutes for the entire duration of the experiment using multi-purpose sensors  
 106 (Flower Power, Parrot SA, Paris, France). This enabled us to adjust watering depending on the degree of local

107 evapotranspiration during the course the experiment. The sensors outside of the tunnel in Madrid (i.e. only  
108 natural rainfall) showed an interquartile range between 1% and 17% soil water content. This overlapped with  
109 the range of 10 to 22% water content of the drought treatment that we artificially imposed inside the tunnels  
110 in Madrid and Tübingen. The lower range of measurements in Madrid (outside sensor) is due to a lack of  
111 natural rainfall during the first two months of the experiment. In contrast, the sensor outside the tunnel in  
112 Tübingen recorded an interquartile range of soil water content percentage of 22 to 27%, which was comparable  
113 to the high watering treatments in Tübingen and Madrid (from 20 to 33%). These values confirmed that our  
114 low and high watering treatment were not only different, but also that they mimicked natural soil water  
115 content at the two contrasting locations. Mean daily air temperatures (measured by the sensors at 5-10 cm  
116 above the soil surface every 15 minutes) were overall higher in Madrid (8-10°C) than in Tübingen (5-6°C), and  
117 the difference in temperature between the sensors inside and outside the tunnels was in both locations on  
118 average only 1°C (Table 1). The photosynthetically active radiation (PAR, wavelengths from 400 to 700 nm) had  
119 a median of 0.1 mol m<sup>-2</sup> day<sup>-1</sup> at night for all experiments. At mid-day (11:00-13.00 hrs), the median PAR in  
120 Madrid was 57.8 mol m<sup>-2</sup> day<sup>-1</sup> outside, and 45.7 mol m<sup>-2</sup> day<sup>-1</sup> inside the tunnel. In Tübingen, the median  
121 values were 29.0 outside, and 30.9 mol m<sup>-2</sup> day<sup>-1</sup> inside the tunnel.

#### 122 **Table 1 Summaries of environmental sensor measurements**

123 A total of 34 sensors were placed in the different treatment blocks (low/high) as well as outside (out) of the foil tunnels  
124 (Fig. 2). The median (interquartile) values of all sensors per treatment and location are shown.

Site	Rainfall	Soil water content (%)	Air temperature (°C)
Madrid	out	14.5 (1.09, 17.46)	8.5 (5.34, 12.39)
Madrid	low	16.1 (11.38, 22.51)	10.0 (6.95, 15.13)
Tuebingen	low	14.7 (10.76, 20.09)	6.6 (3.27, 10.78)
Tuebingen	out	27.7 (22.82, 30.50)	5.6 (2.44, 9.54)
Tuebingen	high	24.6 (20.73, 29.02)	6.6 (3.27, 10.78)
Madrid	high	27.8 (22.62, 33.00)	9.8 (6.82, 15.13)

#### 153 Sowing and quality control

154 During sowing, contamination of neighboring pots with adjacent genotypes can occur for multiple reasons. In  
155 order to avoid such contamination, we chose a day with no wind and sowed seeds at 1-2 cm height from the  
156 soil. Additionally, we took care during the first days to be particularly gentle when using the watering gun to  
157 avoid seed-carryover (bottom watering by flooding was done regularly). We also tried to remove human error  
158 during sowing by preparing and randomizing 2 ml plastic tubes containing the seeds to be sown in the same  
159 layouts (5x8) as the destination trays. During sowing, each experimenter took a box at random and went to the

160 corresponding labeled and arranged tray in the field (Fig. 2). This reduced the possibility of sowing errors.  
161 During vegetative growth, we could identify seedlings that resembled their neighbors or were located in the  
162 border between two pots and removed such plants as potential contaminants. We also used the homogeneity  
163 of flowering within a pot in the population replicates as a further indicator for contamination. When a plant  
164 had a completely different flowering timing or vegetative phenotypes did not coincide with the majority of  
165 plants in the pot, this plant was removed. After sowing and quality control, the total number of pots was  
166 24,747 instead of the original 24,816 pots (99.7%).

## 167 **Field monitoring**

### 168 Image analysis of vegetative rosettes

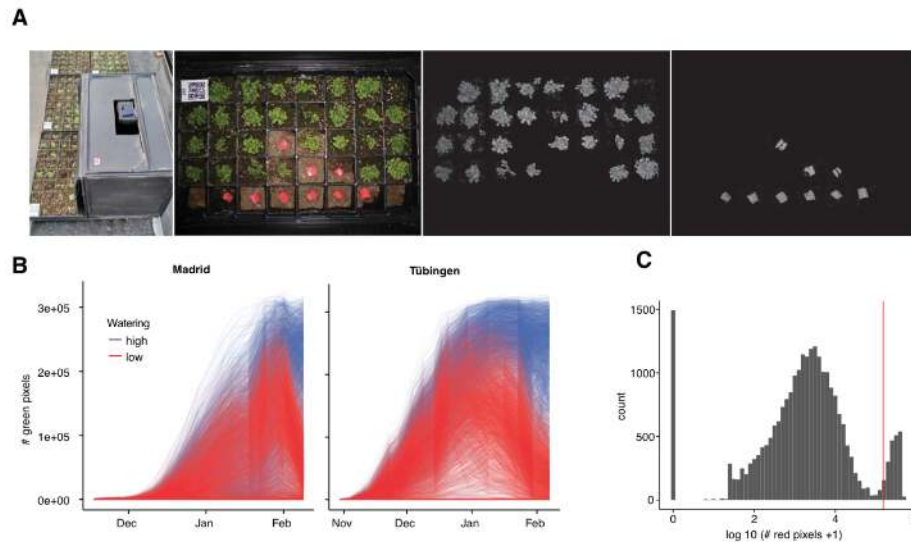
169 Top-view images were acquired every four to five days (median in both sites) with a Panasonic DMC-TZ61  
170 digital camera and a customized closed dark box, the “Fotomatón” (Fig. 3), at a distance of 40 cm from each  
171 tray. In total, we imaged each tray at 20 timepoints throughout vegetative growth. The implemented  
172 segmentation was the same as in Exposito-Alonso et al.<sup>20</sup>, which relies on the Open CV Python library<sup>21</sup>. We  
173 began by transforming images from RGB to HSV channels. We applied a hard segmentation threshold of HSV  
174 values as (H=30-65, S=65-255, V=20-220). The threshold was defined after manually screening 10 different  
175 plants in order to capture the full spectrum of greens both of different accessions and of different  
176 developmental stages. This was followed by several iterations of morphology transformations based on erosion  
177 and dilation. For each of the resulting binary images we counted the number of green pixels.

178 During field monitoring, we noticed that some pots were empty because seeds had not germinated. In  
179 these cases, we left a red marker in the corresponding pots, which could be detected in a similar way as the  
180 presence of green pixels (with threshold H=150-179, S=100-255, V=100-255). These pots were excluded from  
181 survival analysis as they did not contain any plants. An example of transformed images is shown in Fig. 3. The  
182 resulting raw data consist of green and red pixel counts per pot (Fig. 3). In order to detect the red markers  
183 automatically, we performed an analysis of variance between pots above and below a threshold of red pixels  
184 and finding the threshold that maximized this separation. This provided us with the threshold of red pixels  
185 above which a pot had a red marker (indicating an empty pot). As expected, the distribution of pixels was  
186 bimodal, making this identification straightforward (Fig. 3C).

187 We estimated germination timing by analysing trajectories (Fig. 3) of green pixels per pot, and  
188 identifying the first day that over 1,000 green pixels were observed in a pot (corresponding to a plant size of ~



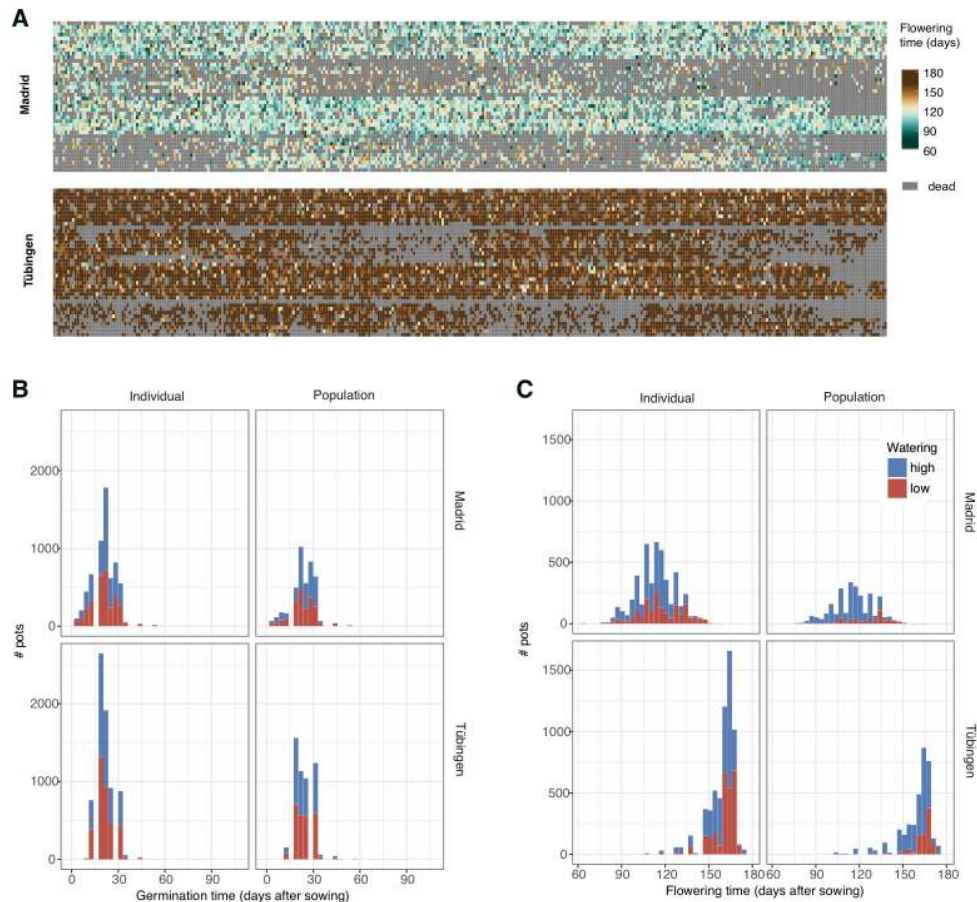
189 10 mm<sup>2</sup>, Fig. 4). The final dataset contained data for 22,779 pots — after the removal of pots with red labels —  
190 with a time series of green pixel counts.



191 **Figure 3. Rosette monitoring.** (A) Customized dark box (“Fotomatón”) for image acquisition and example tray with the  
192 corresponding green and red segmentation. (B) Trajectories of number of green pixels per pot, indicating rosette area, for  
193 Madrid and Tübingen. (C) Distribution of the sum of red pixels per pot over all time frames. The red vertical line indicates  
194 the heuristically chosen threshold to define whether the pot actually had a red marker.

### 195 Manual recording of flowering time

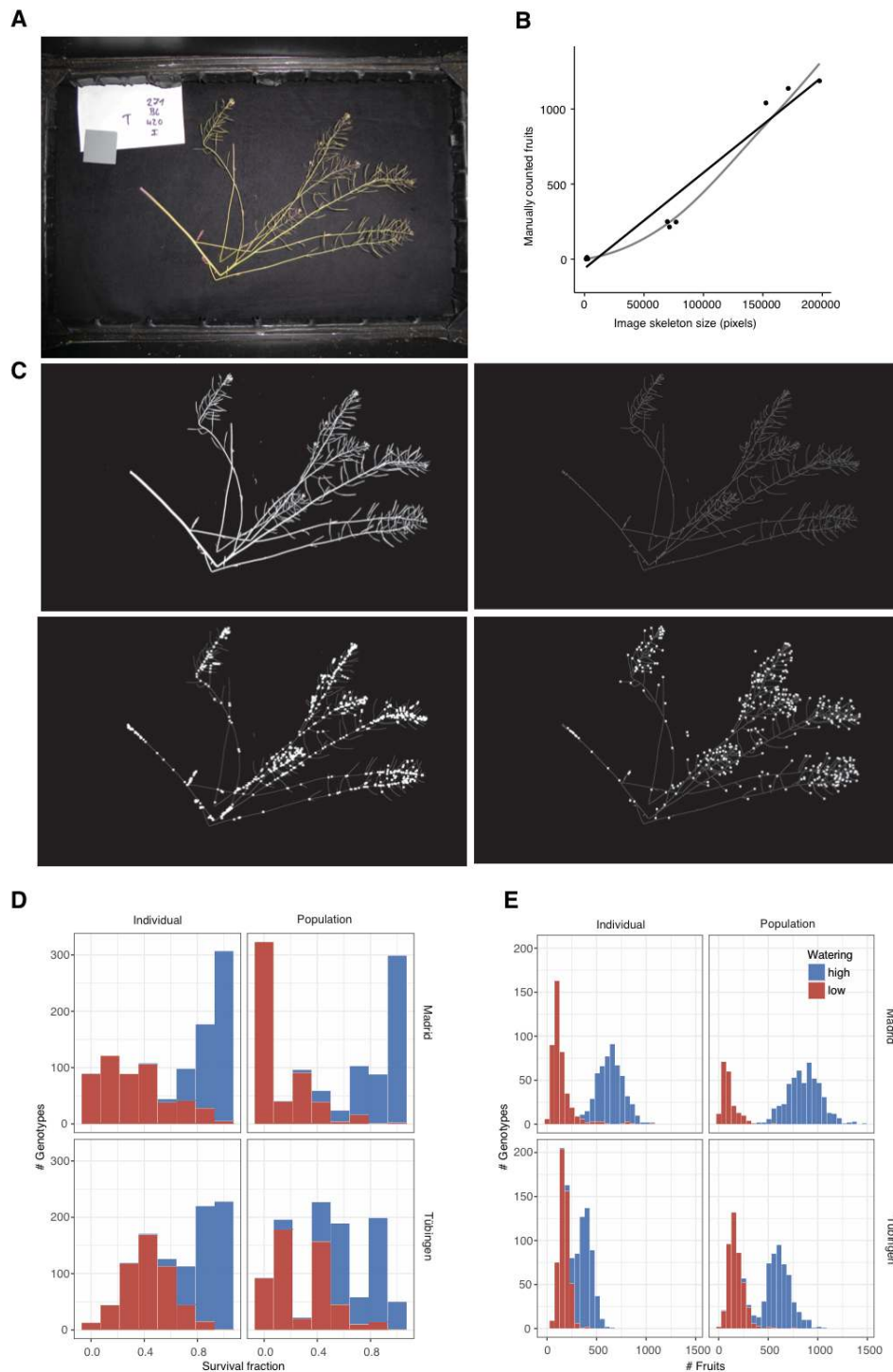
196 We visited the experimental sites every 1-2 days and manually recorded the pots with flowering plants.  
197 Flowering time was measured as the day when the first white petals could be observed with the unaided eye.  
198 This criterion was chosen as sufficiently objective to reduce experimenter error. To keep track of previous visits  
199 and avoid errors, we labeled the pots where flowering had already been recorded with blue pins. To calculate  
200 flowering time, we counted the number of days from the date of sowing to the recorded flowering date (we  
201 did not use the inferred day of germination to avoid introducing modeling errors in the flowering time metric).  
202 Fig. 4 shows the raw flowering time data per pot in the original spatial distribution (Fig. 2) and the distribution  
203 of flowering time per treatment combination. Note that grey boxes in Fig. 4 are pots with plants that did not  
204 survive until flowering. In total, we gathered data for 16,858 pots with flowering plants.



205 **Figure 4. Flowering time distributions.** (A) Flowering times per pot in the same spatial arrangement as in each tunnel (see  
206 Fig. 3). (B) Distribution of germination times. (C) Distribution of flowering times.

207 Image analysis of reproductive plants

208 Once the first dry fruits were observed, we harvested them and took a final 'studio photograph' of the rosette  
209 and the inflorescence (Fig. 5). In total, we took 13,849 photographs. The camera settings were the same as for  
210 the vegetative monitoring, but here we included an 18% grey card approximately in the same location for each  
211 picture in case *a posteriori* white balance adjustments would be needed. We first used a cycle of morphological  
212 transformations of erode-and-dilate to produce the segmented image (Fig. 5). This generated a segmented  
213 white/black image without white noise. Then, we used the thin (erode cycles) algorithm from the Mahotas  
214 Python library<sup>22</sup> to generate a binary picture reduced to single-pixel paths — a process called skeletonisation  
215 (Fig. 5). Finally, to detect the branching points in the skeletonised image we used a hit-or-miss algorithm. We  
216 used customized structural elements to maximize the branch and end point detection (Fig. 5). This resulted in  
217 four variables per image: total segmented inflorescence area, total length of the skeleton path, number of  
218 branching points, and number of end points (Fig. 5).



219 **Figure 5. Inflorescence and seed set estimation.** (A) Representative inflorescence picture. (B) Regression between the  
220 fruits of a few manually counted inflorescences and the inflorescence size calculated based on image processing. The four  
221 variables inferred in (C) accurately predicted the visually counted inflorescences as example ( $R^2=0.97$ ,  $n=11$ ,  $P=10^{-4}$ ). (C)  
222 Resulting variables from image processing of (A): total segmented area (upper-left), skeletonized inflorescence  
223 (upper-right), branching points (lower-left), and endpoints (lower-right). Distribution of survival to reproduction (D) and  
224 fruits per plant (E) in the four environments.

225

### Estimation of fruit and seed number

226 Although the study of natural selection is based on studying relative fitness, and total reproductive area might  
 227 provide a good relative estimate, sometimes it is useful to have a proxy of the absolute fitness. In order to  
 228 provide an approximate number of how many seeds each plant had produced, we generated two allometric  
 229 relationships by visual counting of fruits per plant and seeds per fruit. In order to be sure that the counts  
 230 corresponded to single plants, we counted fruits and seeds of only individual replicates of accessions, not the  
 231 population replicates (see [Field experiment design section](#)). Because a strong relationship had already been  
 232 validated between inflorescence size and the number of fruits in a number of studies with *A. thaliana*<sup>23–25</sup>, we  
 233 decided that counting a few inflorescences of three sizes, reflecting the broad size spectrum, would be  
 234 sufficient to establish a first allometric relationship with the four image-acquired variables (n=11  
 235 inflorescences,  $R^2=0.97$ ,  $P=4\times 10^{-4}$ , [Fig.5B,C](#)). To express fecundity as the number of seeds, we counted all  
 236 seeds inside one fruit for each of the inflorescences used for the first allometric relationship (n=11 fruits),  
 237 aiming for a wide range of fruit sizes. The mean was 28.3 seeds per fruit and the standard deviation was 11.2  
 238 seeds. The two aforementioned allometric relationships were used to predict, first, the number of fruits per  
 239 inflorescence using the four image analysis variables, and second, the number of seeds corresponding to the  
 240 number of fruits per inflorescence.

241

### **Data records**

242 The main datasets of accession information and trait values measured in the field for all replicates as well as  
 243 curated averages per genotype are available as supplementary information at [xxx](#). The datasets are also part of  
 244 the R package “dryAR” available at <http://github.com/MoisesExpositoAlonso/dryAR> with doi [xxx](#).

245

### **Table 2 Variable descriptions**

246 Variable names and their descriptions and units are reported. All datasets share a common accession identification  
 247 number.

Dataset	Variable	Information
D1&D2&2D3&D4	id	Unique numeric ID assigned to the accessions included in the 1001 Genomes Project
D1&D2	name	Classic accession name assigned by original collector
D1&D2	country	Country of collection
D1&D2	sitename	Toponym of the location of collection
D1&D2	latitude	Degrees North of the location of origin (°N)
D1&D2	longitude	Degrees East of the location of origin (°E)
D1&D2	collector	Original researcher that collected the accession
D1&D2	collectiondate	Calendar date of collection
D1&D2	CS_number	Stock number in the Arabidopsis Biological Resource Center ( <a href="http://abrc.osu.edu">abrc.osu.edu</a> )
D1&D2	Q_SNPcongruency	Pass/no pass of thresholds for genome quality and SNP calling congruency
D1&D2	Q_geneticsdist	Pass/no pass of the filter for almost identical accessions

D1&D2	Q_geodist	Pass/no pass of filter for geographically close accessions
D1&D2	is_relict	Belongs to the Mediterranean "relict" lineage
D1&D2	finalset	Included in the final 517 set for the field experiment
D3&D4	site	Field station site. m=Madrid(Spain), t=Tübingen(Germany)
D3&D4	water	Rainfall/watering treatment. h=high rainfall, l=low rainfall
D3&D4	indpop	Density of plants per pot. i=single plant selected after germination, 4p=population of 30 seeds growing undisturbed
D3&D4	qpblock	Identification number of quickpot (tray) within treatment block (rainfall row x 8 replicate block ) (see Fig. 2)
D3&D4	qp	Identification number of quickpot tray in the whole experiment
D3&D4	qp_x	Pot position in x axis within the quickpot tray
D3&D4	qp_y	Pot position in y axis within the quickpot tray
D3&D4	pos	Pot x,y coordinate within the quickpot tray
D3&D4	rep	Replicate number
D3&D4	trayid	Identification of the tray combining block and treatments
D3&D4	potindex	Identification of pot combining site, tray, and position within the tray
D3&D4	Germination_time	Inference of germination time based on the day that rosette area was over 31,000 pixels size (days after sowing)
D3&D4	Green	Sum of all green areas per pot throughout the experiment (# pixels). This 7 helps to identify successfully growing pots.
D3&D4	Red	Sum of all red areas per pot throughout the experiment (# pixels). This helps 1 to identify red tags placed on pots that failed throughout the experiment
D3&D4	Survival_flowering	Survival until reproduction (i.e. production of flowers)
D3&D4	Flowering_date	Date that the first flowers had developed
D3&D4	Flowering_time	Time from sowing until the date of flowering (days)
D3&D4	Inflorescence_size	Area of inflorescence (#pixels)
D3&D4	Survival_num	Number of surviving plants until fruit set. Only applies to "population" pots.
D3&D4	Survival_fruit	Survival until fruit set (i.e. produced fruits)
D3&D4	Fruits	Number of fruits inferred from the function between visually counted fruits 3 and inflorescence area, total path, branching points, and ending points.
D3&D4	Seeds	Number of seeds inferred from the average number of seeds per fruit and 7 number of fruits.
D3&D4	Infloresncence_byind	Area of inflorescence (#pixels) divided by total number of plants per pot. Only 1 applies to "population" pots.
D3&D4	Fruits_byind	Number of fruits divided by total number of plants per pot. Only applies to 5 "population" pots.
D3&D4	Seeds_byind	Number of seeds divided by total number of plants per pot. Only applies to 9 "population" pots.
D3&D4	Fitness	Lifetime fitness (number of seeds / seed planted). This metric integrates 3 survivorship and reproduction.

## 384 Technical validation

### 385 Data processing

386 All images are deposited at [\[updatehere\]](#). The Python modules to process images for green area segmentation  
 387 and inflorescence analyses are available at <http://github.com/MoisesExpositoAlonso/hippo> and  
 388 <http://github.com/MoisesExpositoAlonso/hitfruit>, along with example datasets.

389 To reproduce our data curation procedure we created the R package dryAR  
390 (<http://github.com/MoisesExpositoAlonso/dryAR> with doi xxx). All scripts to re-generate data from raw files  
391 can be found at <http://github.com/MoisesExpositoAlonso/dryAR/data-cleaning>.

### 392 Replicability of image processing

393 After testing different camera parameters, we used an exposure of -2/3 and an ISO of 100. White balance was  
394 set for flashlight. We used a dark box with all sides closed, so the flashlight was the only source of illumination.  
395 This ensured that the white balance and illumination were virtually consistent from picture to picture, as  
396 shown before<sup>20</sup>. Photos were saved both in .jpeg and .raw to allow for *a posteriori* adjustments if needed.  
397 Using a calibration board with 1.3 cm x 1.3 cm white and dark squares, we examined the error between the  
398 inferred area from image analysis and the real 1.3 cm-side squares across the tray. This provided us with a  
399 median resolution estimate of 101.5 pixels mm<sup>-2</sup>. The deviations from the true area were minimal, with a  
400 median of 2.7% and values of 1.4% / 4.2% for the 1<sup>st</sup> and 3<sup>rd</sup> quartile. The maximum area deviations were of 8  
401 to 9% in the extreme corners of the tray, where we did not sow any seeds. We are confident that such small  
402 variation in retrieved area is compensated by the randomized locations of genotypes within the trays.

403 To further verify that our camera settings and segmentation pipeline produced replicable extractions of  
404 plant green area, we used images of trays that were photographed twice on the same day by mistake. In total  
405 there were 1,508 such pots distributed across 11 timepoints and different trays. By comparing the area of the  
406 same pot of two different camera shots and segmentation analyses, we could verify that the Spearman's rank  
407 correlation was very high ( $r=0.97$ ,  $n=1508$ ,  $P<10^{-16}$ ), confirming high replicability.

408 Because we ran the same segmentation and skeletonization software on both rosette and  
409 inflorescence images, we could leverage the clearly different image patterns that rosettes and inflorescences  
410 have to identify labeling errors (i.e. mistakes in manually inputting sample information of the pictures). To do  
411 this, we first trained a random forest model to predict the manually labeled "rosette" or "inflorescence" by the  
412 four image variables in Fig. 5. By fitting a Random Forest with all images, we find that the leave-one-out  
413 accuracy was 92.1%, i.e. ca. 2,000 images were incorrectly labeled by the algorithm. We manually checked  
414 whether these were mislabeled or rather whether they "looked similar" in terms of area or landmark points in  
415 the photo, e.g. when both rosette or inflorescences were diminute. We found that only 2.5% were incorrectly  
416 mislabeled (and corrected them) and are thus confident that the labeling error must be below 2.5%.

### 417 Experimental validation

418 Although repeating experiments in climatically-similar locations would be impractical, we could verify that  
419 survival in Madrid and low precipitation correlated with a preliminary drought experiment in the greenhouse  
420 (Spearman's  $\rho=0.17$ ,  $n=211$ ,  $P=0.01$ )<sup>20</sup>. On the other hand, reproductive allocation measured under optimal  
421 conditions in the greenhouse correlated with total seed output in the most similar field experiments, Tübingen  
422 high precipitation (Spearman's  $\rho=0.27$ ,  $n=211$ ,  $P=5 \times 10^{-5}$ )<sup>23</sup>.

## 423 **ADDITIONAL INFORMATION**

### 424 **Acknowledgements**

425 We are thankful to Belen Mendez-Vigo, Carlos Alonso-Blanco and the technical service at CBGP-UMP, Antolín  
426 López Quirós, Marisa López Herránz and Miguel Ángel Mora Plaza, for assistance during sowing in Madrid. We  
427 also thank Xavi Picó for advice on experimental design.

428 **Supplementary Information** accompanies this paper at [xxx](#)

429 **Competing interests:** The authors declare no competing financial interests.

430 **Funding statement** This work was funded by an ERC Advanced Grant IMMUNEMESIS and the Max Planck  
431 Society (DW).

### 432 **Author contributions**

433 MEA conceived and designed the project. MEA carried out the experiment in Tübingen. MEA and RGR carried  
434 out the experiment in Madrid. All authors contributed to specific tasks in the experiments (see detailed  
435 description below). OB provided the field site in Tübingen and FGA provided the site in Madrid. DW secured  
436 funding for the project. MEA carried out the analyses and wrote the first draft of the manuscript. All authors  
437 edited, commented and approved the manuscript.

AUTHOR	Conceived_idea	Funding	Advice	Coordination	Materials	Bulking_seeds	Seed_aliquoting	Field_setup	Pictures_plants	Sowing_Madrid	Sowing_Tuebingen	Thinning_seedlings	Field_care	Image_processing	Foil_tunnel_reparation	Fresh_harvesting_Madrid	Fresh_harvesting_Tuebingen	Dry_imaging_Madrid	Dry_imaging_Tuebingen	Flowering_monitoring	Image_processing	Data analysis/processing	Writing
Moises Exposito-Alonso	x			x	x	x	x	x	x	x	x	x	x	x	x	x	x	x	x	x	x	x	x
Rocio Gomez Rodriguez							x	x	x	x			x	x		x				x		x	
Detlef Weigel		x	x		x													x					
Hernán A Burbano			x							x													
Oliver Bossdorf			x		x																		
Rebecca Schwab			x	x	x													x					
Fernando García Arenal			x		x																		
George Wang			x																				
François Vasseur			x								x												
Julian Regalado							x																
Derek Lundberg											x							x					
Ronja Wedegärtner							x	x	x		x		x					x					
Frank Weiss									x														
Danelle Seymour											x												
Beth Rowan											x				x		x						
Patricia Lang									x		x	x			x	x	x						
Jorge Kagayema											x												
Rui Wu											x				x		x						
Wanyan Xi											x												
Kavita Venkataramani											x				x	x	x						
Giovanna Capovilla												x			x		x						
Efthymia Symeonidi								x				x			x		x						
Vera Middendorf												x							x	x			
Anna-Lena Van de Weyer												x											
Jane Devos												x											
Diep Thi Ngoc Tran												x											
Sonja Kersten					x						x				x								
Wangsheng Zhu															x								
Maricris Zaidem															x								
Sebastian Petersen																							
Ezgi Dogan																							
Claudia Friedemann																							
Talia Karasov																							
Cristina Barragán																							
Leily Rabbani																							
Caspar Gross																							
Lukas Reinelt																							
Eunyoung Chae																							

438 **Datasets**

439 **Dataset 1 Quality-based selection of the original 1,135 accessions**

440 We report the 1001 Genome identification numbers, the quality filters that each accession passed during the  
441 selection of the 517 set.

442 **Dataset 2 Description of the 517 accessions**

443 We report the final set of 517 accessions that were used in the field experiment.

444 **Dataset 3 All traits measured per replicate**

445 For each pot replicate, we report all raw data as well as composite variables.

446 **Dataset 4 Curated means per accession**

447 For each accession, we report all data as well as composite variables.



448 **REFERENCES**

- 449
1. Darwin, C. *The Origin of Species*. (John Murray, 1859).
  - 450 2. Fisher, S. R. A. *The genetical theory of natural selection*. (The Clarendon Press, 1930).
  - 451 3. Hereford, J. A quantitative survey of local adaptation and fitness trade-offs. *Am. Nat.* **173**, 579–588 (2009).
  - 452 4. Kingsolver, J. G. *et al.* The strength of phenotypic selection in natural populations. *Am. Nat.* **157**, 245–261
  - 453 (2001).
  - 454 5. Siepielski, A. M. *et al.* The spatial patterns of directional phenotypic selection. *Ecol. Lett.* **16**, 1382–1392
  - 455 (2013).
  - 456 6. Siepielski, A. M., DiBattista, J. D. & Carlson, S. M. It's about time: the temporal dynamics of phenotypic
  - 457 selection in the wild. *Ecol. Lett.* **12**, 1261–1276 (2009).
  - 458 7. Thurman, T. J. & Barrett, R. D. H. The genetic consequences of selection in natural populations. *Mol. Ecol.*
  - 459 **25**, 1429–1448 (2016).
  - 460 8. Gompert, Z. *et al.* Experimental evidence for ecological selection on genome variation in the wild. *Ecol.*
  - 461 *Lett.* **17**, 369–379 (2014).
  - 462 9. Anderson, J. T., Lee, C.-R. & Mitchell-Olds, T. Strong selection genome-wide enhances fitness trade-offs
  - 463 across environments and episodes of selection. *Evolution* **68**, 16–31 (2014).
  - 464 10. Dai, A. Increasing drought under global warming in observations and models. *Nat. Clim. Chang.* **3**, 52–58
  - 465 (2012).
  - 466 11. Hoffmann, A. A. & Sgrò, C. M. Climate change and evolutionary adaptation. *Nature* **470**, 479–485 (2011).
  - 467 12. Tielbörger, K. *et al.* Middle-Eastern plant communities tolerate 9 years of drought in a multi-site climate
  - 468 manipulation experiment. *Nat. Commun.* **5**, 5102 (2014).
  - 469 13. 1001 Genomes Consortium. 1,135 Genomes Reveal the Global Pattern of Polymorphism in *Arabidopsis*
  - 470 *thaliana*. *Cell* **166**, 481–491 (2016).
  - 471 14. Burghardt, L. T., Young, N. D. & Tiffin, P. A Guide to Genome-Wide Association Mapping in Plants. *Current*

- 472 *Protocols in Plant Biology* 22–38 (2017).
- 473 15. Milcu, A. *et al.* Genotypic variability enhances the reproducibility of an ecological study. *Nat Ecol Evol* **2**,  
474 279–287 (2018).
- 475 16. Exposito-Alonso, M., Burbano, H. A., Bossdorf, O., Nielsen, R. & Weigel, D. A map of climate change-driven  
476 natural selection in *Arabidopsis thaliana*. *bioRxiv* 321133 (2018). doi:10.1101/321133
- 477 17. Seren, Ü. *et al.* AraPheno: a public database for *Arabidopsis thaliana* phenotypes. *Nucleic Acids Res.* **45**,  
478 D1054–D1059 (2017).
- 479 18. Atwell, S. *et al.* Genome-wide association study of 107 phenotypes in *Arabidopsis thaliana* inbred lines.  
480 *Nature* **465**, 627–631 (2010).
- 481 19. Purcell, S. *et al.* PLINK: a tool set for whole-genome association and population-based linkage analyses.  
482 *Am. J. Hum. Genet.* **81**, 559–575 (2007).
- 483 20. Exposito-Alonso, M. *et al.* Genomic basis and evolutionary potential for extreme drought adaptation in  
484 *Arabidopsis thaliana*. *Nat Ecol Evol* **2**, 352–358 (2018).
- 485 21. Itseez. Open Source Computer Vision Library. (2015). Available at: <https://github.com/itseez/opencv>.
- 486 22. Coelho, L. P. Mahotas: Open source software for scriptable computer vision. *Journal of Open Research*  
487 *Software* **1**, e3 (2013).
- 488 23. Vasseur, F., Wang, G., Bresson, J., Schwab, R. & Weigel, D. Image-based methods for phenotyping growth  
489 dynamics and fitness in *Arabidopsis thaliana*. *bioRxiv* (2018).
- 490 24. Brachi, B. *et al.* Coselected genes determine adaptive variation in herbivore resistance throughout the  
491 native range of *Arabidopsis thaliana*. *Proceedings of the National Academy of Sciences* **112**, 4032–4037  
492 (2015).
- 493 25. Roux, F., Gasquez, J. & Reboud, X. The dominance of the herbicide resistance cost in several *Arabidopsis*  
494 *thaliana* mutant lines. *Genetics* **166**, 449–460 (2004).